Climate change, in the framework of the constructal law

M. Clausse

Laboratoire de Génie des Procédés pour l'Environnement,
l'Energie et la Santé (LGP2ES - EA 21),
CNAM, ICENER, case 2D3P20,
292 rue St. Martin, 75141 Paris Cedex 03, France

and

ESIEE Paris, 2 boulevard Blaise Pascal Cité DESCARTES,
BP 99 93162, Noisy le Grand CEDEX, France
E-mail: marc.clausse@cnam.fr

F. Meunier

Laboratoire de Génie des Procédés pour l'Environnement,
l'Energie et la Santé (LGP2ES - EA 21),
CNAM, ICENER, case 2D3P20,
292 rue St. Martin, 75141 Paris Cedex 03, France
E-mail: meunierf@cnam.fr

A.H. Reis*

Department of Physics and Evora Geophysics Centre,
University of Évora, Ramalho,
59, 7000-67 1 Evora, Portugal
E-mail: ahr@uevora.pt
*Corresponding author

A. Bejan

Department of Mechanical Engineering and Materials Science,
Duke University, Durham,
NC 27708-0300, USA
E-mail: abejan@duke.edu

Abstract: Here we present a simple and transparent alternative to the complex models of earth's thermal behaviour under time-changing conditions. We show the one-to-one relationship between changes in atmospheric properties and time-dependent changes in temperature and its distribution on earth. The model accounts for convection and radiation, thermal inertia and changes in albedo (ρ) and greenhouse factor (γ). The constructal law is used as the principle that governs the evolution of flow configuration on earth. The model showed that for two time-dependent scenarios, (δ_ρ=0.002; δ_γ=0.011) and (δ_ρ=0.002; δ_γ=0.005) the predicted equatorial and polar temperature increases and the time scales are (ΔT_H=1.16 K; ΔT_L=1.11 K; 104 years) and (0.41 K;

0.41 K; 57 years), respectively. A continuous model of temperature variation was used to predict the thermal response of the Earth's surface to changes bounded by $\delta_\rho = \delta_\gamma$ and $\delta_\rho = -\delta_\gamma$. The poleward heat current reaches its maximum in the vicinity of 35° latitude, accounting for the position of the Ferrel cell between the Hadley and Polar Cells.

Reference to this paper should be made as follows: Clausse, M., Meunier F., Reis, A.H. and Bejan, A. (2012) 'Climate change, in the framework of the constructal law', *Int. J. Global Warming*, Vol. 4, Nos. 3/4, pp.242–260.

Biographical notes: Marc Clausse received his engineer and MSc degrees form INSA de Lyon (1998) and his PhD from CNAM de Paris in 2003. He is currently Associate Professor at ESIEE Paris and his research focuses on sorption processes for gas separation (CO_2 capture) and energy conversion, energy efficiency, and more generally the impact of energy use on environment.

Francis Meunier graduated at Ecole Polytechnique Paris. He got his PhD in Solid State Physics (superconductivity) from the Université Paris Sud. He shifted towards solar energy and more generally energy related topics (in particular adsorption heat pumps) in 1977. In 1994, he joined, as a Professor, the Conservatoire National des Arts et Métiers in Paris where his research activity is dedicated to energy and its impact on environment including climate change.

Antonio Heitor Reis graduated with a degree in Physics from the University of Lisbon and received his MSc in Mechanical Engineering from the Technical University of Lisbon (IST) and his PhD in Physics from the University of Évora, Portugal. From 1981 until 1986, he did research on energy at the National Laboratory for Engineering and Technology. He joined the University of Évora in 1986, where he teaches Physics and Engineering courses. He is currently the Director of the Évora Geophysics Centre of the University of Évora. His current research interests comprise energy issues, atmospheric physics, flows in porous media (animate and inanimate) and constructal theory.

Adrian Bejan received all his degrees from MIT BS (1971, Honors Course), MS (1972, Honors Course) and PhD (1975). His research is in Thermodynamics, Applied Physics, and the Constructal Law of Design and Evolution in Nature. He is ranked by ISI among the 100 most-cited authors in all of Engineering (all fields, all countries, living or deceased). He is the author of 25 books and 550 peer-refereed journal articles. His h index on ISI is 47. Professor Bejan was awarded 16 honorary doctorates from universities in 11 countries, for example the Swiss Federal Institute of Technology (ETH Zurich) and the University of Rome I 'La Sapienza'. He received numerous international awards for thermal sciences.

1 Introduction

In this paper, we present in simple terms the relationship between changes in average atmospheric properties and time-dependent changes in the distribution of temperature on earth. We focus on the predictable relationship between these two phenomena, not on what may cause changes in the atmosphere. We show that if atmospheric changes are known or predicted, climate response is predictable in concise and transparent terms.

Two recent articles (Bejan and Reis, 2005; Reis and Bejan, 2006) showed how to use the constructal law to predict the essential features of global climate and atmospheric and oceanic circulation. This was demonstrated in simple and direct terms (with pencil and paper) by combining the constructal law with a simple model of the earth as a heat engine connected to a brake, i.e., an engine with zero delivery of mechanical power to an external user. In accordance with the constructal law, the access of the convective heat current flowing from the warm zone of the earth to the cold zones was maximised. This was achieved by properly sizing the areas of the warm and cold zones, i.e., by generating the configuration (the design) of the flow system and from this were derived the basic climate features, which match observations.

The work described in Bejan and Reis (2005) and Reis and Bejan (2006) was based on steady-state and quasisteady (periodic, diurnal) models. Its success recommends its application to elucidating what is perhaps the biggest issue in geophysics today: climate change, its time scale and how to make its treatment and understanding accessible with pencil and paper, or chalk on the blackboard. In this article, we unveil the relationship between changes in the radiative properties of the atmosphere (albedo, greenhouse factor) and time-dependent changes in the global climate. The key features of this relationship are the time scale and magnitude of the changes.

Before plunging into details, we draw attention to the two significant bodies of literature to which this new work belongs. First, the constructal law has been applied with success to predict patterns in nature in many domains other than global climate, for example, river basins scaling, the distribution of human settlements in geography, animal locomotion (running, flying, swimming, sports evolution), dendritic solidification, turbulent flow structure, human dynamics (e.g., urban design, city traffic), allometric scaling in biology, cracks in shrinking solids, dendritic aggregation of dust particles, heterogeneous multiscale porous media, etc. This literature was reviewed in Bejan (1997, 2000, 2006), Reis (2006) and Bejan and Lorente (2006).

Second, in geophysics there is a significant body of work based on ad hoc invocations of optimality, for example, Maximum Entropy Production (MEP) in Malkus (1954), Lorenz (1955), Paltridge (1975, 1978), Schulman (1977), North (1981), Lin (1982), Swenson (1989) and Lorenz et al. (2001). This work was reviewed in Reis and Bejan (2006) and Whitfield (2006) and is not reviewed again here. It suffices to say that the constructal law is different from MEP because the constructal law is a general statement of physics, about a physics *phenomenon* that had been overlooked: the time evolution (generation) of flow configuration (design). It is not about the end result (max, min, or optimal), but about the time direction of the evolution phenomenon itself. It applies across the board, from geophysics to biology, engineering and social dynamics.

The constructal law was proposed as a self-standing law of physics in 1996: "For a finite-size flow system to persist in time (to live), its configuration must change in such a way that it provides easier and easier access to the currents that flow through it" (Bejan, 1997). The direction of the 'movie tape' of flow configuration evolution is the law: existing flow configurations are being replaced in time by easier flowing configurations.

2 Model

We use the model proposed in Reis and Bejan (2006) (see Fig. 1). The surface temperature is quasi-steady: it is averaged over many daily cycles and annual cycles, but it changes slowly with the changes in the radiative properties of the atmosphere. The surface is not isothermal:

it is divided into an equatorial zone of area A_H and temperature $T_H(t)$ and a polar zone of total area A_L and temperature $T_L(t)$. The total surface is fixed.

$$A_H + A_L = A = 4\pi R^2 \tag{1}$$

where R is the earth's radius. In the following analysis, we use the dimensionless area fraction x, which is defined as

$$x = \frac{A_H}{A} \qquad (1-x) = \frac{A_L}{A}. \tag{2}$$

Figure 1 Earth model with warm (A_H) and cold (A_L) zones and latitudinal convective heat current between them

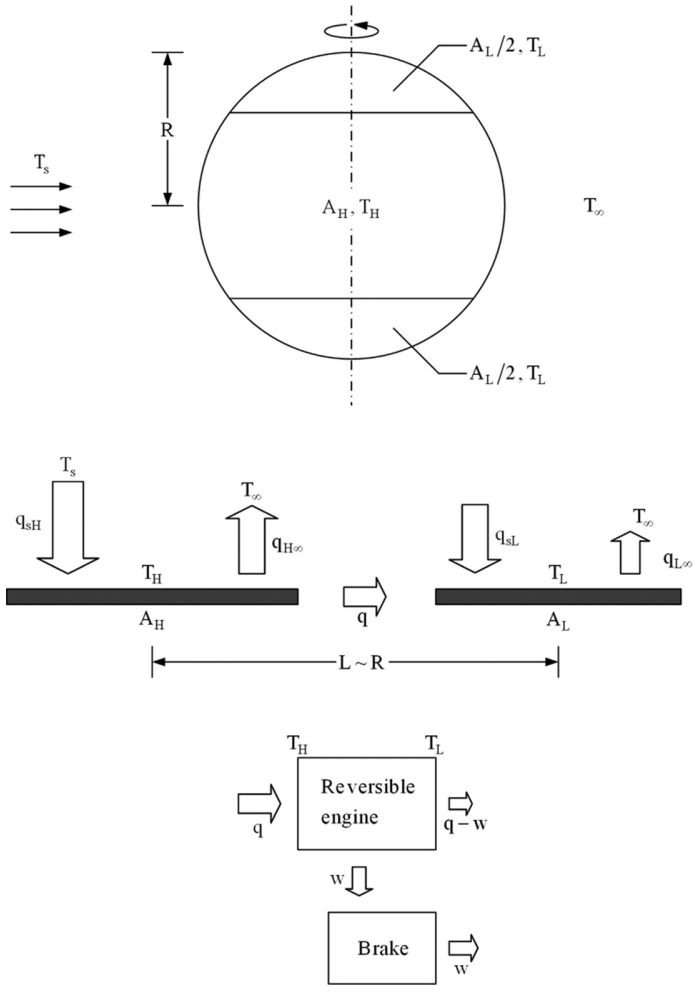

The thermal inertia of the earth's crust is modelled as a layer of ocean water of average depth h (equal to 2750 m), which covers the entire globe. This h value is obtained by taking the

total volume of ocean water and dividing it by the earth's surface area. This model of earth's thermal inertia finds support in the fact that the observed earth's energy balance since 1950 shows that almost all energy surplus is stored in the ocean (Domingues et al., 2008; Murphy et al., 2009). The mass of the body of water covering A_H is then $M_H = \rho_w A_H h$ and in the polar zone $M_L = \rho_w A_L h$, where ρ_w is the density of water. Consequently, we also have $M = M_H + M_L$, constant, where $M_H/M = x$.

By invoking the first law of thermodynamics for M_H, we obtain

$$M_H c\left(\frac{dT_H}{dt}\right) = q_{sH} - q_{H\infty} - q, \tag{3}$$

where c is the specific heat of water and q is the heat transfer rate between M_H and M_L. The radiation heat transfer model is the same as in De Vos (1992) and De Vos and Van der Wel (1993). The equatorial surface receives the solar heat current

$$q_{sH} = A_{Hp}(1-\rho) f_H \sigma T_S^4, \tag{4}$$

where T_s, σ, f_H and ρ are the temperatures of the sun as a black body (5762 K), the Stefan Boltzmann constant (5.67×10^{-8} $\mathrm{Wm^{-2}\,K^{-4}}$), the earth–sun view factor (2.16×10^{-5}) and the albedo of the earth ($\rho = 0.299$, in the period 2000–2004, see Trenberth et al., 2009). The area A_{Hp} is the area A_H projected on a plane perpendicular to the direction earth–sun. The ratio A_{Hp}/A_H decreases from $1/\pi$ when A_H is a narrow belt along the equator, to 1/4 when A_H covers the globe completely:

$$\frac{A_{Hp}}{A_H} = f_H = \frac{\theta + \sin\theta\cos\theta}{2\pi \sin\theta}. \tag{5}$$

Here θ is the latitude of the transition from A_H to A_L, with $\theta = 0$ is at the equator and $\theta = \pi/2$ at the north pole (Fig. 1).

The A_H surface radiates into space the heat current

$$q_{H\infty} = A_H(1-\gamma)\sigma T_H^4, \tag{6}$$

where $\gamma \sim 0.4$ is the earth's greenhouse factor, or the reflectance in the infrared region ($\gamma = 0.397$ in the period 2000–2004, see Trenberth et al., 2009).

The first law for the M_L portion of the crust requires

$$M_L c\left(\frac{dT_L}{dt}\right) = q_{sL} + q - q_{L\infty}. \tag{7}$$

The radiative heat current received from the sun, q_{sL}, is a new feature that is added to the model of Bejan and Reis (2005):

$$q_{sL} = A_{Lp}(1-\rho) f_L \ \sigma T_S^4. \tag{8}$$

The radiation current transmitted to the cold background is $q_{L\infty}$,

$$q_{L\infty} = A_L(1-\gamma)\sigma T_L^4. \tag{9}$$

The projected area of the polar zone is related to the area of the polar zone by:

$$\frac{A_{Lp}}{A_L} = f_L = \frac{\pi/2 - \theta - \sin\theta\cos\theta}{2\pi(1-\sin\theta)}. \tag{10}$$

Equations (6) and (9) have been simplified by neglecting T_∞^4 in favour of T_H^4 and T_L^4, respectively.

Finally, the heat current q is driven from T_H to T_L by the buoyancy effect in the layer of fluid that covers the earth's surface. As shown in Bejan and Reis (2005), to derive the q formula we neglect factors of order 1, in accordance with the rules of scale analysis (Bejan, 2004). The fluid layer covers an area of flow length $L(\sim R)$ and width $W(\sim R)$. The vertical length scale of the fluid layer, H, will be defined shortly. The length L bridges the gap between T_H and T_L.

At the T_H-end of the fluid layer, the hydrostatic pressure at the bottom of the layer is $\rho_H gH$. Similarly, at the T_L-end, the pressure is $\rho_L gH$. The pressure difference in the L direction is:

$$\Delta P \approx \left(\rho_L - \rho_H\right) gH \approx \rho\beta\left(T_H - T_L\right)\mathrm{gH}, \tag{11}$$

where ρ is the mean fluid density and β is the coefficient of volumetric thermal expansion.

The fluid-layer control volume is exposed to the force ΔPWH in the L direction. This force is opposed by the shear force felt by the moving fluid over the surface LW,

$$\Delta PWH = \tau LW. \tag{12}$$

The average shear stress is

$$\tau \approx \rho\varepsilon_M \frac{u}{H}, \tag{13}$$

where ε_M is the eddy diffusivity for momentum and u is the velocity in the L direction. For the order of magnitude of ε_M, we use Prandtl's mixing length model (e.g., Bejan, 2004, p. 343), in which we take H to represent the mixing length,

$$\varepsilon_M = H^2 \frac{u}{H} = Hu. \tag{14}$$

In other words, H is the vertical dimension of the fluid system that mixes (transfers momentum vertically) while moving horizontally. Note that H is not the vertical extent of the fluid layer. By eliminating ΔP, u and ε_M between equations (11)–(14), we obtain the horizontal velocity scale

$$u \approx \left[\beta g\left(T_H - T_L\right)\frac{H^2}{L}\right]^{1/2}. \tag{15}$$

The convective heat transfer rate associated with the counter-flow between T_H and T_L depends on whether the two branches of the counter-flow are in intimate thermal contact. They are not if the circulation is in the plane $L \times W$, as in the case of R-scale oceanic and atmospheric currents that complete loops over large portions of the globe (Fig. 2a). Another example is when the loop is a vertical plane aligned with the meridian, when the branches of the counter-flow are far enough apart and do not exchange heat in a significant way in the vertical direction (Fig. 2b). In such cases, the convective heat current is

$$q \approx \rho u H W c_p \left(T_H - T_L\right), \tag{16}$$

or, after using equation (15) and $L \sim W \sim R$,

$$q \approx \rho c_p \left(g\beta\right)^{1/2} H^2 R^{1/2} \left(T_H - T_L\right)^{3/2}. \tag{17}$$

Figure 2 Convection loops in the fluid layer connecting the warm and cold zones

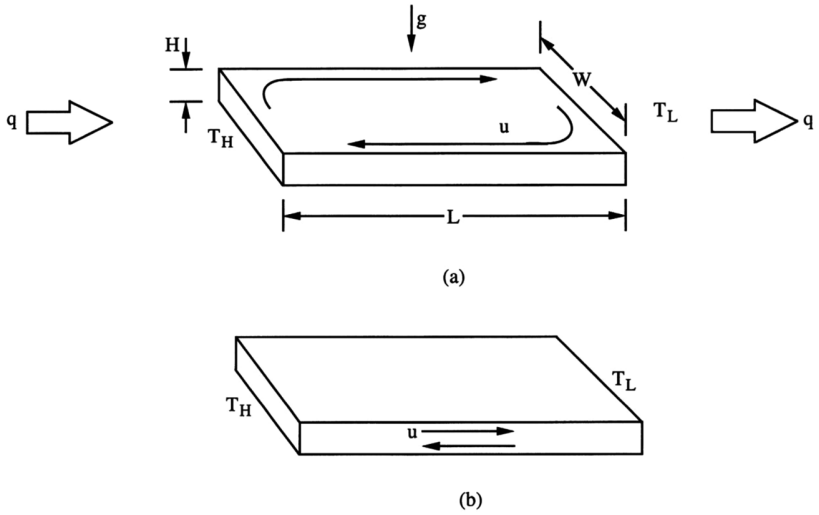

According to the constructal law, the configuration that will prevail is the one that provides progressively greater conductance for the flow of q. It was shown in Bejan and Reis (2005) that greater access is provided by the second configuration (Fig. 2b); therefore, in this paper, we rely on equation (17) to estimate the rate of heat convection from M_H to M_L.

Note further that in writing equations (3) and (7), we treated M_H and M_L as closed systems. This is permissible because the net mass flow affected by the counter-flow (Fig. 2) is zero and because the enthalpy current carried by the counter-flow (q) is analogous to a heat current across a surface with zero mass flow (cf. Bejan, 2006, p.512).

3 Numerical formulation

The dimensionless formulation of the governing equations is based on using the following scales

$$T_{\text{scale}} = f^{1/4} T_s = 392.8 \text{ K}, \tag{18}$$

$$t_{\text{scale}} = \frac{\rho_w hc}{\sigma T_{\text{scale}}^3}, \tag{19}$$

where h is the average depth of the layer of ocean water, as defined in Section 2. The dimensionless variables are:

$$\left(\tilde{T}_H, \tilde{T}_L\right) = \frac{\left(T_H, T_L\right)}{T_{\text{scale}}}, \tag{20}$$

$$\tilde{t} = \frac{t}{t_{\text{scale}}}, \tag{21}$$

$$\tilde{q} = \frac{q}{\sigma T_{\text{scale}}^4 A}, \tag{22}$$

Equations (3), (7) and (17) become

$$x\left(\frac{d\tilde{T}_H}{d\tilde{t}}\right) = xf_H(1-\rho) - x(1-\gamma)\tilde{T}_H^4 - \tilde{q}, \tag{23}$$

$$(1-x)\left(\frac{d\tilde{T}_L}{d\tilde{t}}\right) = (1-x)f_L(1-\rho) + \tilde{q} - (1-x)(1-\gamma)\tilde{T}_L^4, \tag{24}$$

$$\tilde{q} \approx C\left(\tilde{T}_H - \tilde{T}_L\right)^{3/2}, \tag{25}$$

where C is the group,

$$C = \frac{\rho c_p \left(g\beta\right)^{1/2} H^2 R^{1/2}}{\sigma A T_{\text{scale}}^{5/2}}. \tag{26}$$

If we use $H \sim 2$ km for the thickness of the mixing layer in the atmosphere at 0º C, $R \sim 6600$ km and $A = 4\pi R^2$, then C ~ 0.04. On the other hand, the conductance $C_{3/2}$ in Bejan and Reis (2005) corresponds to the assumption that $H \sim 5.2$ km, in which case $C \sim 0.181$. The numerical results reported in the next section are based on $C = 0.181$.

In summary, there are three equations [equations (23)–(25)] containing four unknowns $\left(\tilde{T}_H, \tilde{T}_L, \tilde{q}, x\right)$, which are functions of time. The radiative parameters are assumed specified. The problem is closed by invoking the constructal law, which states that the design of the flow system evolves toward greater flow access for the heat current from the hot zone to the cold zone,

$$\partial\tilde{q}/\partial x = 0. \tag{27}$$

The evolution toward greater flow access is achieved by selecting the configuration, which is represented by x.

4 Simulation of global warming and cooling

Changes in the albedo (ρ) and the earth's greenhouse factor (γ) are caused by many processes on the earth's surface, including human activity. What causes these changes is not the phenomenon addressed in this paper. The problem is to determine the response of the

global climate when the ρ and γ are known (e.g., measured, or predicted with confidence). The sequence of numerical simulations described next was designed to test the response of the global climate parameters $\left(\tilde{T}_H, \tilde{T}_L, x\right)$ to changes in the radiative properties of the atmosphere (ρ, γ).

To start with, as reference configuration we generated the steady state that prevails when $\rho = 0.3$ and $\gamma = 0.4$. This state is determined by solving equations (23), (24), (25) and (27) with $d/d\tilde{t} = 0$ in equations (23) and (24). The results are

$$\begin{aligned} &\rho = 0.3 \qquad && x = 0.8401 \\ &\gamma = 0.4 \qquad && \tilde{T}_H = 0.7471 (T_H = 293.5\,K) \\ & && \tilde{T}_L = 0.6577 (T_L = 258.4\,K). \end{aligned} \tag{28}$$

The average surface temperature $\overline{T} = 293.5 \times 0.8401 + 258.4 \times (1 - 0.8401) = 288.3$ K (15.2ºC) which is close to the actual value (~18ºC).

The value found for x corresponds to the latitudes 57° N and 57° S. Therefore, the polar zones predicted in this paper are wider than the commonly known polar zones, which correspond to the latitudes 66°37 N and S.

4.1 Step changes in albedo and greenhouse factor

One common feature of all such simulations is that the optimal area ratio x is a function of t, ρ and γ. For the step change, x will be set at its new steady state value, assuming that the area partitioning the equatorial and the polar zones instantaneously adapts to the new values of ρ and γ.

Two step changes in the albedo and the greenhouse factor are considered: (*A*) $\delta_\rho = 0.002$ with $\delta_\gamma = 0.011$ and (*B*) $\delta_\rho = 0.002$ with $\delta_\gamma = 0.005$ (Fig. 3). Four time scales are plotted: one for the non-dimensional time and three others corresponding to different ratios of ocean layer mass taken into account for earth's inertia (case 1: 100%, case 2: 50% and case 3: 33%).

For case (*A*), the new steady state calculated on the basis of the model in Section 3 is represented by

$$\begin{aligned} &\rho = 0.302 \qquad && x = 0.8398 \\ &\gamma = 0.411 \qquad && \Delta T_H = 1.16\,K \\ & && \Delta T_L = 1.11\,K, \end{aligned} \tag{29}$$

while for case (*B*), it is represented by

$$\begin{aligned} &\rho = 0.302 \qquad && x = 0.8395 \\ &\gamma = 0.405 \qquad && \Delta T_H = 0.41\,K \\ & && \Delta T_L = 0.41\,K. \end{aligned} \tag{30}$$

The overall mean temperature change is 1.15 K for case (*A*) and 0.41 K for case (*B*). The time needed for the earth's mean temperature to reach 60% of its equilibrium response is $\tilde{t} = 0.98$ for case (*A*) and $\tilde{t} = 0.91$ for case (*B*). Depending on the mass fraction of ocean layer taken into account in the inertia calculation, these times correspond to 104, 57 and 35 years for cases 1, 2 and 3, respectively.

Figure 3 Earth's energy flux imbalance and temperature increase for the polar zone (ΔT_L) and the equatorial zone (ΔT_H) evolutions in response to two different step changes in albedo (ρ) and greenhouse factor (γ). Four time scales are plotted: non dimensional time and three cases corresponding to different ratio of ocean layer mass taken into account for earth's inertia (case 1: 100%, case 2: 50% and case 3: 33%) (see online version for colours)

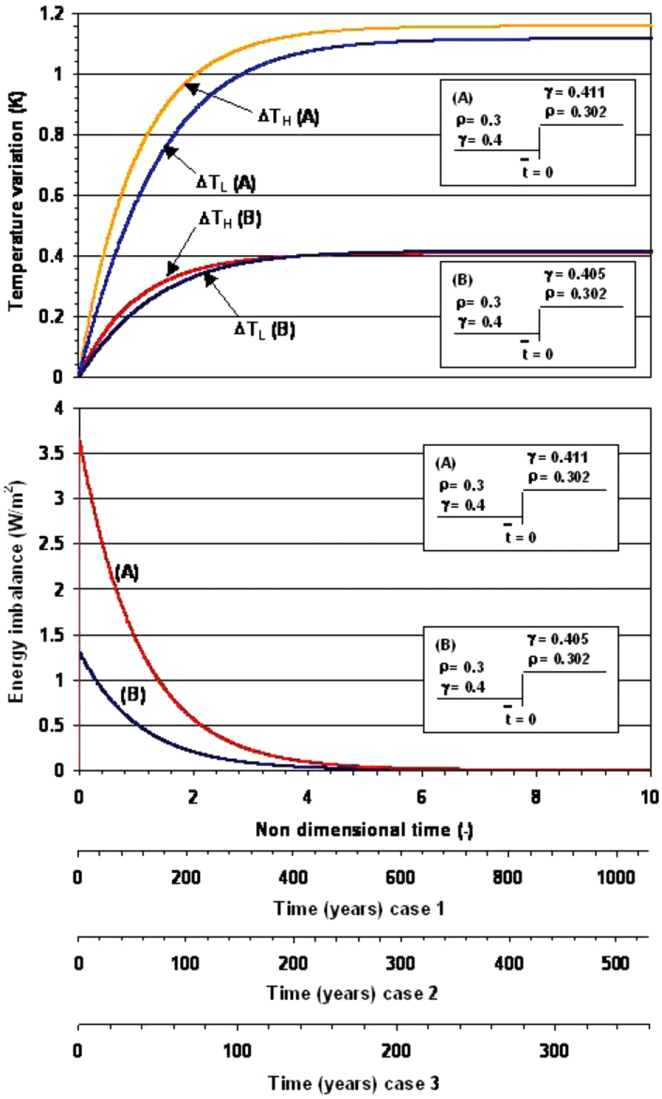

The evolution of the earth's energy imbalance is also reported in Figure 3. The energy imbalance is defined as the net heat current received from the sun ($q_{sH}+q_{sL}$) minus the net heat current rejected to the outer space ($q_{H\infty}+q_{L\infty}$):

$$q''_{ex}=\left[(q_{sH}+q_{sL})-(q_{H\infty}+q_{L\infty})\right]/A. \tag{31}$$

The energy imbalance is the highest initially [3.67 W/m^2, case (A)], while it is still significant [1.47 W/m^2, case (A)] when 60% of the temperature response is reached. Although coming

from a simple model, these results are consistent with those based on highly complex meteorological models. For example, using the global climate model of the NASA Goddard Institute of Space Studies to simulate the climate evolution for the 1880–2003 period, Hansen et al. (2005) have found an overall temperature increase of 1.2 K for an increase of 0.6 K after 120 years. The same authors report an energy imbalance reaching 0.85 ± 0.15 W/m^2 for an overall energy imbalance of 1.8 W/m^2 relative to 1880. Furthermore, 25–50 years are needed for the earth's temperature to reach 60% of its equilibrium response. Hansen et al. (2005) also reported that 85% of the heat storage occurs above 750 m depth. The depth taken into account for thermal inertia calculation in case 3 (917 m) is of the same order of magnitude, so that only case 3 is studied in what follows.

4.2 Ramp function for ρ and γ increase

To improve the model, a linear increase of ρ and γ lasting 120 years is assumed. The initial and final values of ρ and γ are maintained at the same levels as those used in Section 4.1. The x value is optimised at every time step during the evolution of ρ and γ.

The temperature and energy imbalance evolutions are presented on Figure 4 by assuming that the earth's inertia is equal to one-third of the ocean mass (cf. case 3 in Section 4.1).

Figure 4 Earth's energy flux imbalance and temperature increase for the polar zone (ΔT_L) and the equatorial zone (ΔT_H) evolutions in response to two different ramp changes in albedo (ρ) and greenhouse factor (γ) (see online version for colours)

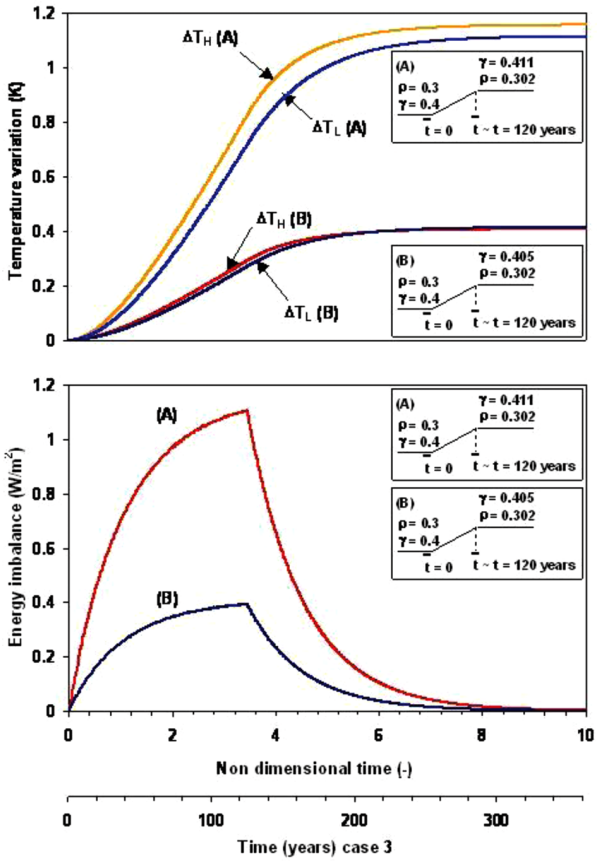

The steady states are the same as those reported in Section 4.1 and equations (29) and (30). At $t = 120$ years and for a γ increase of 0.011, the temperature increase is 0.7 K for the polar zone, while it reaches 0.81 K for the equatorial zones. Comparing with results found by Hansen et al. (2005), our calculated values are in relatively good agreement with those found by these authors: 0.77 K for the mean temperature increase and 1.1 W/m^2 for the energy imbalance in our case compared to 0.6 K and 0.85 W/m^2, respectively for about the same period of time.

As the values of γ and ρ were kept constant after 120 years, the results obtained after that date could be compared to those found by Wigley (2005) for his Constant Concentration (CC) scenario. In his case, the reference year is 2000, which in our case corresponds to an elapsed time of 120 years.

If we compare the results at year 2200 (i.e., an elapsed time of 320 years in our case), our calculations match Wigley' results quite well for the case of the CC scenario: case (A) is close to his central climate sensitivity scenario (0.36 K compared to 0.33 K, respectively) while case (B) is close to the low sensitivity scenario (0.13 K compared to 0.15 K).

4.3 Continuous increases in ρ and γ

In this section, we present the results for a continuous linear increase of γ and ρ. The rates are equal to those used in Section 4.2, case (A). This model gives an idea of the earth's response to a 'business as usual' scenario. Two scenarios are considered:

- Case (A), the rates of increase for γ and ρ are equal to their respective values used in Section 4.2:

$$\gamma = 0.4 + \frac{0.011 \cdot \tilde{t}}{3.45} \text{ and } \rho = 0.3 + \frac{0.002 \cdot \tilde{t}}{3.45}.$$

This represents an optimistic view for γ, as it is known that the CO_2 emission rate has greatly increased in the past 50 years. Hence, the IEA (2008) reports global emissions equal to 20,945 Mtons/y of CO_2 in 1990, 27,889 Mtons/y in 2006 but 40,553 Mtons/y are foreseen in 2030. To improve our model, a change in the rate for γ (doubling), starting at year 2000, is implemented and corresponds to case (B):

- Case (B) is identical to case (A) for $\tilde{t} \le 3.45$ (~120 years) and above this value, the γ increase rate is multiplied by a factor of two: $\gamma = 0.4 + \frac{0.022 \cdot (\tilde{t} - 3.45)}{3.45}$ and $\rho = 0.3 + \frac{0.002 \cdot \tilde{t}}{3.45}$ for $\tilde{t} > 3.45$.

The origin of time still corresponds to the year 1880, as was the case in Section 4.2. Figure 5 shows that after 320 years, the mean temperature increase is roughly 2.5 K for case (A) and 4.3 K for case (B). For the period between 120 and 320 years, this corresponds to an increase of 1.88 K and 3.75 K for cases (A) and (B), respectively. Comparing these last results with the values found by Wigley (2005) in his Constant Emissions (CE) scenario at year 2200, case (B) is slightly above the Wigley's value for high climate sensitivity to CO_2 doubling (3.3 K), while case (A) is almost equal to the value found by Wigley for medium climate sensitivity (2.1 K).

Figure 5 Earth's energy flux imbalance and temperature increase for the polar zone (ΔT_L) and the equatorial zone (ΔT_H) evolutions in response to a continuous change (constant emission scenario) in albedo (ρ) and greenhouse factor (γ) (see online version for colours)

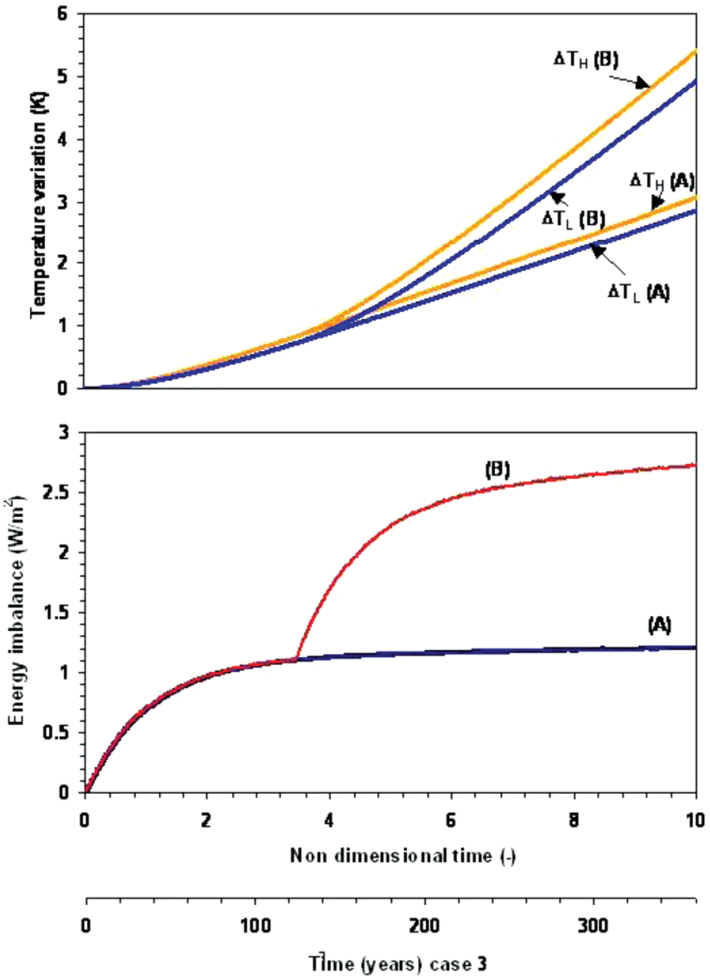

Another reading of Figure 5 is to evaluate the remaining time before reaching a temperature increase of 2 K, above which value the consequences on climate are seen to be irreversible. This threshold is reached after 200 and 250 years for cases (A) and (B), respectively. Hence, measured from today, there remain 70 years in the worst case before reaching the 2 K increase. Lowering the CO_2 emissions to a rate close to that between years 1880 and 2000, would result in a 50 years delay only.

Concerning the energy imbalance, it is evaluated by Wigley (2005) at 3.7 W/m^2 for a CO_2 doubling. The values found based on our model 1.2 W/m^2 and 2.7 W/m^2 remain below those of Wigley. However, the comparison between these values is not straightforward, as Wigley's value is achieved for CO_2 concentration doubling, whereas in our case, the energy imbalance depends on ρ and γ evolutions.

5 Continuous earth temperature model

In this section, we examine more closely the heat flow in the poleward direction and how this flow depends on the albedo (ρ) and the earth's greenhouse factor (γ). Consider an infinitesimal ring of radius $R\cos\theta$. The width of the earth's surface at the latitude θ is $Rd\theta$. The area perpendicular to the sunrays is $2R^2\cos^2\theta d\theta$ (see Fig. 6). The heat balance in such a ring requires:

$$2R^2 f(1-\rho)\sigma T_s^4\cos^2\theta d\theta - 2\pi R^2(1-\gamma)\sigma T^4\cos\theta d\theta - dq = 0, \tag{32}$$

Figure 6 Heat flows in a control surface ring at latitude θ: q_s represents the solar radiation absorbed at the surface, q_∞ is terrestrial radiation emitted into the outer space and q is the imbalanced heat flow convected over the earth's surface

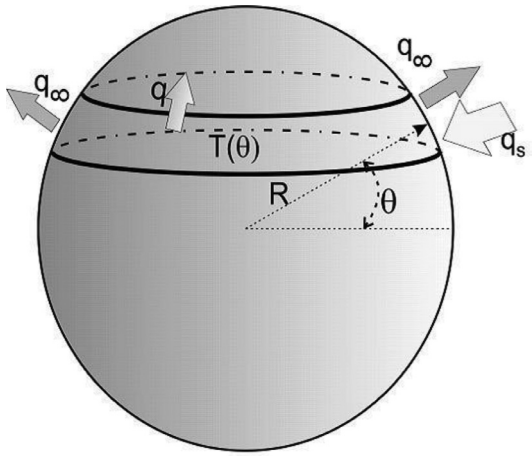

where all the symbols have the same significance as in the preceding sections. The excess heat current q in the ring is convected toward the poles (the cold sinks) by the earth's global circulation. Therefore, the variation of the poleward heat flow with latitude is given by:

$$dq/d\theta = 2R^2\sigma\cos\theta\left\lfloor f(1-\rho)T_s^4\cos\theta - \pi(1-\gamma)T^4\right\rfloor. \tag{33}$$

The heat flow at the latitude θ is obtained by integrating equation (33) from 0 to θ:

$$q(\theta) = \int_0^\theta 2R^2\sigma\left[f(1-\rho)T_s^4\cos^2\theta - \pi(1-\gamma)T^4\cos\theta\right]d\theta. \tag{34}$$

By using the mean value of T^4, it is possible to estimate the hemispheric poleward heat current as:

$$q(\theta) \approx 2R^2\sigma\left[f/2(1-\rho)T_s^4\left(\sin(2\theta)/2+\theta\right) - \pi(1-\gamma)\overline{T}^4\sin\theta\right] \tag{35}$$

Because $q(\theta)$ must be zero at the pole, equation (35) offers the opportunity to evaluate the average surface temperature $\overline{T}$. Therefore, with $\theta = \pi/2$ and assuming $\overline{T}^4 \sim \left(\overline{T}\right)^4$ (note

that the error involved here is of order $12\sigma_T^2/(\overline{T})^2 \sim 0.06$, where σ_T is the standard error), equation (35) yields

$$\overline{T} \sim \left[\frac{f(1-\rho)}{4(1-\gamma)}\right]^{1/4} T_s. \tag{36}$$

Additionally, symmetry requires $dq/d\theta = 0$ at the equator. Therefore, we obtain the equator temperature from equation (32) as:

$$T_{eq} = \left[\frac{f(1-\rho)}{\pi(1-\gamma)}\right]^{1/4} T_s. \tag{37}$$

By using $\rho = 0.3$ and $\gamma = 0.4$, we obtain $\overline{T} \sim 288.7$ K (15.5ºC), which is close to the actual value (~18ºC) and $T_{eq} = 306.7\ K$ (33.5ºC), which is also close to the observed value. A rough estimate of the pole temperature is $T_p \approx 2\overline{T} - T_{eq} = 270.7\ K$ (−3.1ºC), which corresponds to a temperature difference of 36 *K* between equator and pole.

Both $q(\theta)$ and $dq/d\theta$ are presented in Figure 7. We see that q has a maximum close to the latitude 35º and it drops to zero at the equator and the poles. In the representation of $dq/d\theta$, a linear estimate of the local temperature $T(\theta) \approx T_{eq} - 2\theta/\pi \cdot (T_{eq} - T_p)$ has been used. We observe that between the equator and latitude 35º, the earth's surface contributes positively to the poleward heat flow, while from latitude 35° onwards, the earth's surface absorbs heat from that flow.

Figure 7 Poleward heat flow and its variation with latitude. Note that from the equator onto the latitude 35º, heat is continuously added to the heat flow q, while heat is removed from q between latitude 35° and the pole

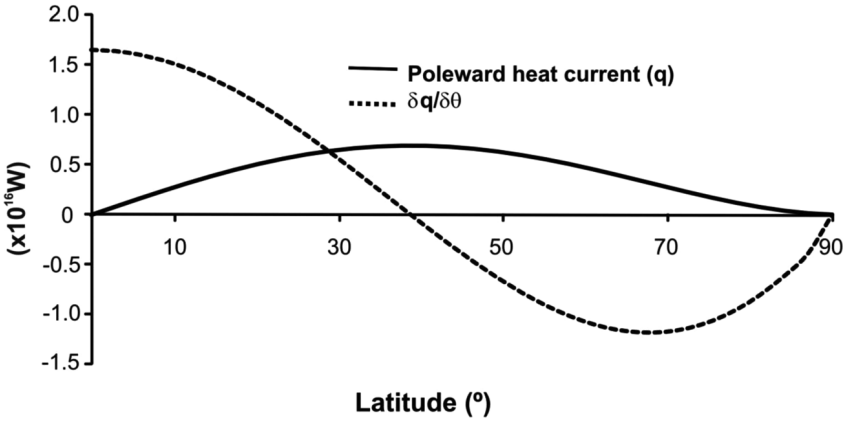

The current increase in aerosol concentration in the atmosphere leads to an increase in the cloud cover (Givati and Rosenfeld, 2004), which, combined with the direct effect of light reflection by aerosols, increases the albedo ρ of the earth. As a consequence, less solar radiation is absorbed at the surface. On the other hand, the increasing concentration of greenhouse gases has the effect of impeding the escape of terrestrial radiation into space,

thus increasing the greenhouse factor γ. The trade-off between these opposing trends results in a net positive radiative imbalance of order $q''_{ex} = 0.85$ W/m^2 (Hansen et al., 2005).

The sensitivity of the average surface temperature to changes in ρ and γ can be calculated from equation (36) and is plotted in Figure 8 for both cases in which ρ and γ have the same and opposite sign of variation. We see that the effect on temperature is higher when ρ and γ vary in opposite directions. The actual trend must correspond to a curve between these two extremes and must stay close to the curve $d\rho = d\gamma$.

Figure 8 Average surface temperature as function of the earth's greenhouse factor for variations of the albedo with the same and opposite sign of the variations of the earth's greenhouse factor

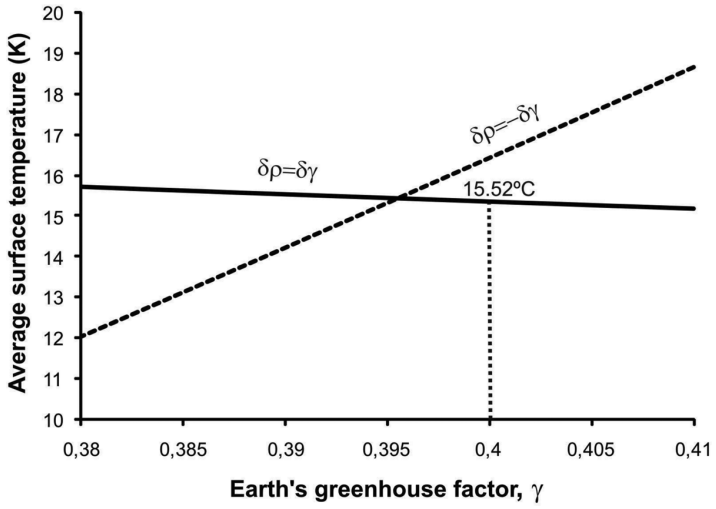

By invoking the constructal law, we can anticipate the effect of these trends on the earth's temperature along the meridian. At every latitude θ the heat flow [equation (34)] depends on the albedo ρ and greenhouse factor γ (which are constrained) and temperature T (which is the free parameter). The constructal law requires maximum heat flow at all latitudes; therefore, by maximising $q(\theta)$ of equation (34), we obtain

$$\delta T = \left[\overline{T}/(1-\gamma)\right]\left[-(f\cos\theta/4\pi)(T_s/T)^4\,\delta\rho + (1/4)\,\delta\gamma\right]. \tag{38}$$

The latitudinal temperature variation for various cases is shown in Figure 9. Here, we used the average temperature based on equation (35). The variations $\delta\rho \sim 0-0.002$ and $\delta\gamma \sim 0.005$ generate positive temperature changes of order 0.6 K, which match the observed value corresponding the past 100 years (IPCC Synthesis Report, 2007).

Except for the cases in which the albedo maintains its current value, the changes in the surface temperature vary with latitude and show higher temperature increase in the polar regions. This effect reduces the equator-to-pole temperature difference, thereby reducing the poleward heat flow [equation (17)]. This reduction is shown in Figure 10 for the case in which $\delta_\rho = 0.002$ and $\delta_\gamma = 0.005$ and amounts to –2.7% (see Figures 7 and 10). Furthermore, the larger temperature increase in the polar regions (~0.2ºC) is consistent with the actual reduction in iced areas around the poles. Note also that the reduction in the solar radiation absorbed at the surface is of order $\delta_\rho/(1-\rho) \sim 0.3\%$ [equation (4)].

Figure 9 Changes of the surface temperature with latitude for various changes in the albedo and the earth's greenhouse factor. The variations $\delta_\rho = 0 - 0.002$ and $\delta_\gamma = 0.005$ generate changes in surface temperature of order 0.6ºC that is the observed value. Latitudinal changes are due to changes in the albedo solely

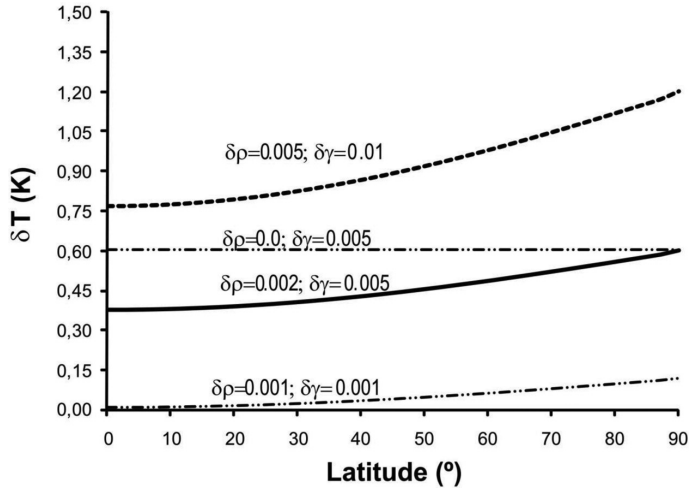

Figure 10 Reduction of the poleward heat flow as a function of latitude due to increase in the albedo and the earth's greenhouse factor ($\delta_\rho = 0.002$ and $\delta_\gamma = 0.005$)

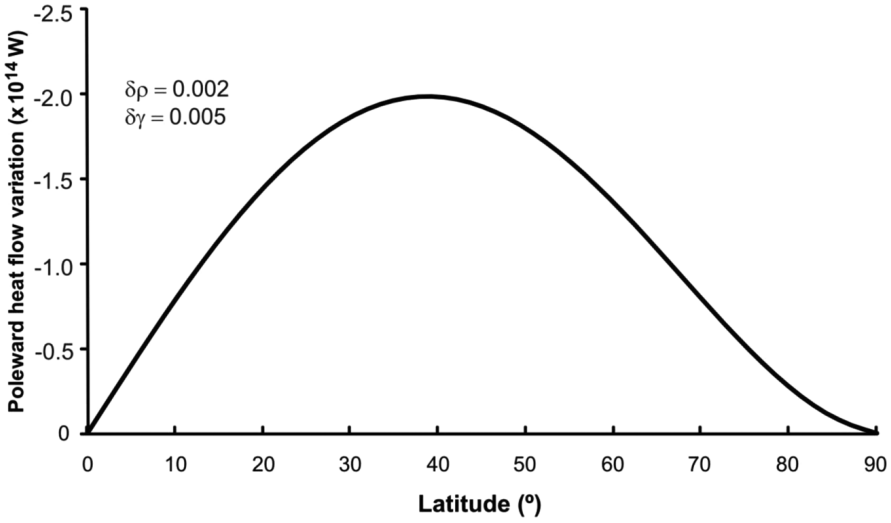

The poleward heat flow calculated with equation (34) (and Fig. 7) at the latitudes 25º and 53º that represent the boundaries between the Hadley and Ferrel cells and the Ferrel and polar cells, has practically the same values as those resulting from the constructal configuration of the global circulation (Bejan and Reis, 2006). The heat flow values calculated based on equation (34) are $q_{25^\circ} \sim 5.5 \times 10^{15}\,\mathrm{W}$ and $q_{53^\circ} \sim 6 \times 10^{15}\,\mathrm{W}$, while those presented in Bejan and Reis (2006) are $q_{25^\circ} \sim 4.5 \times 10^{15}\,\mathrm{W}$ and $q_{53^\circ} \sim 6.2 \times 10^{15}\,\mathrm{W}$, respectively.

6 Conclusions

Complex models of the earth's thermal behaviour are opaque from the point of view of the general audience and contain the uncertainties of the many flows of various scales that are included in these models. Given this background, simple models provide interesting results, even if with fewer details. In this paper, a simple convection/radiation model was used for anticipating the time-dependent response of the earth's climate to changes in the albedo and greenhouse factors. The novelty is the simplicity and transparency and the use of constructal law as the principle that governs the evolution of flow configuration in time and provides closure of the model equations.

In the first part of the paper, the model was tested for the actual state of the earth, by using the measured values of the earth's albedo and greenhouse factors. The results were consistent with the actual thermal state of the earth and the equator to pole temperature difference. The thermal response of the earth was then tested for changes in the earth's albedo and greenhouse factors, namely ($\delta_\rho = 0.002$; $\delta_\gamma = 0.011$) and ($\delta_\rho = 0.002$; $\delta_\gamma = 0.005$). The results indicated that equatorial and polar temperatures increase by ($\Delta T_H = 1.16$ K ; $\Delta T_L = 1.11$ K) and ($\Delta T_H = 0.41\ K$; $\Delta T_L = 0.41$ K), respectively. The time needed for the earth's mean temperature to reach 60% of its equilibrium response is 104 and 57 years, respectively, while the radiative imbalance is of the same order as the measured value (0.85 ± 0.15 W/m^2).

In the second part of the paper, we used a continuous model of changing atmospheric radiative properties. These values, determined for the equator and polar temperatures and the equatorial to pole temperature difference, are consistent with the actual values. A continuous mapping of earth forcing through changes in albedo and greenhouse factors was obtained for the domain between $\delta_\rho = \delta_\gamma$ and $\delta_\rho = -\delta_\gamma$. It was shown that the values of the actual global warming are consistent with forcing amplitudes close to $\delta_\rho = 0.002$ and $\delta_\gamma = 0.005$. An additional result is that the poleward heat current reaches its maximum close to the latitude 35°, therefore indicating that between this latitude and the pole, the earth's thermal budget is negative. This latitude corresponds to the position of the Ferrel cell in the global circulation, which is driven by the Hadley cell that exports heat and the Polar cell, which acts as heat receiver.

Acknowledgements

A.H. Reis' work was supported by Fundação para a Ciência e Tecnologia (Portugal) under the project PTDC/EME-MFE/71960/2006. Adrian Bejan's contribution was supported by grants from the US National Renewable Energy Laboratory (Golden, Colorado) and the US Air Force Office of Scientific Research.

References

Bejan, A. (1997) *Advanced Engineering Thermodynamics*, 2nd ed., Wiley, New York, ch. 13.

Bejan, A. (2000) *Shape and Structure, from Engineering to Nature*, Cambridge University Press, Cambridge, UK.

Bejan, A. (2004) *Convection Heat Transfer*, 3rd ed., Hoboken.

Bejan, A. (2006) *Advanced Engineering Thermodynamics*, 3rd ed., Wiley, Hoboken.

Bejan, A. and Reis, A.H. (2005) 'Thermodynamic optimization of global circulation and climate', *International Journal of Energy Research*, Vol. 29, pp.303–316.

Bejan, A. and Lorente, S. (2006) 'Constructal theory of generation of configuration in nature and engineering', *Journal of Applied Physics*, Vol. 100, pp.1–27.

Domingues, C.M., Church, J.A., White, N.J., Gleckler, P.J., Wijffels, S.E., Barker, P.M. and Dunn, J.E. (2008) 'Improved estimates of upper-ocean warming and multi-decadal sea-level rise', *Nature*, Vol. 453, pp.1090–1093.

De Vos, A. (1992) *Endoreversible Thermodynamics of Solar Energy Conversion*, Oxford University Press, Oxford, UK, pp.53–67.

De Vos, A. and Van der Wel, P. (1993) 'The efficiency of the conversion of solar energy into wind energy by means of Hadley cells', *Theor. Appl. Climatol*., Vol. 46, pp.193–202.

Givati A. and Rosenfeld, D. (2004) 'Quantifying precipitation suppression due to air pollution', *Journal of Applied Meteorology*, Vol. 43, pp.1038–1056.

Hansen, J. *et al.* (2005) 'Earth's energy imbalance: confirmation and implications', *Science*, Vol. 308, No. 3, pp.1431–1434.

IEA World Energy Outlook (2008) *International Energy Agency Report*, Paris, http://www.iea.org/textbase/nppdf/free/2008/weo2008.pdf (Accessed 20 August 2012).

IPCC Synthesis Report (2007) http://www.ipcc.ch/pdf/assessment-report/syr/ar4_syr.pdf

Lin, C.A. (1982) 'An extremal principle for a one-dimensional climate model', *Geophysical Research Letters*, Vol. 9, pp.716–718.

Lorenz, E.N. (1955) 'Available potential energy and the maintenance of the general circulation', *Tellus*, Vol. 7, pp.157–167.

Lorenz, R.D., Lunine, J.I., McKay, C.P. and Withers, P.G. (2001) 'Titan, Mars and Earth: entropy production by latitudinal heat transport', *Geophysical Research Letters*, Vol. 25, pp.415–418.

Malkus, W.V.R. (1954) 'The heat transport and spectrum of turbulence', *Proc. R. Soc. Ser. A*, Vol. 225, pp.196–212.

Murphy, D.M., Solomon, S., Portmann, R.W., Rosenlof, K.H., Forster, P.M. and Wong, T. (2009) 'An observationally based energy balance for the Earth since 1950', *Journal of Geophysical Research*, Vol. 114, DOI:10.1029/2009JD012105, pp.D17107.

North, G.R. (1981) 'Energy balance climate models', *Reviews of Geophysics and Space Physics*, Vol. 19, pp.91–121.

Paltridge, G.W. (1975) 'Global dynamics and climate—a system of minimum entropy exchange', *Quart. J. R. Met. Soc*., Vol. 101, pp.475–484.

Paltridge, G.W. (1978) 'The steady-state format of global climate', *Quart. J. R. Met. Soc.*, Vol. 104, pp.927–945.

Reis, A.H. (2006) 'Constructal theory: from engineering to physics and how flow systems develop shape and structure', *Applied Mechanics Reviews*, Vol. 59, pp.269–282.

Reis, A.H. and Bejan, A. (2006) 'Constructal theory of global circulation and climate', *International Journal of Heat and Mass Transfer*, Vol. 49, pp.1857–1875.

Schulman, L.L. (1977) 'A theoretical study of the efficiency of the general circulation', *J. Atmospheric Sciences*, Vol. 34, pp.559–580.

Swenson, R. (1989) 'Emergent attractors and a law of maximum entropy production: foundations to a theory of general evolution', *Systems Research*, Vol. 6, pp.187–197.

Trenberth, K.E., Fasullo, J.T. and Kiehl, J. (2009) 'Earth's global energy budget', *Bulletin of the American Meteorological Society*, (March), Vol. 90, pp.311–323.

Whitfield, J. (2006) 'Order out of chaos', *Nature*, Vol. 436, No. 7053, pp.905–907.

Wigley, T.M.L. (2005) 'The climate change commitment', *Science*, Vol. 307, pp.1766–1769.